ELSEVIER

Surface Science 382 (1997) 275–287

surface science

Local electric field effects in STM of single-atom adsorption on a Si(001) surface

Anna Pomyalov, Yishay Manassen *

Department of Chemical Physics, The Weizmann Institute of Science, Rehovot 76100, Israel

Received 11 April 1996; accepted for publication 13 February 1997

Abstract

The effect of the tip-induced electric field on STM images and spectra from a Si(001) surface on which Sb, Na and K atoms were adsorbed at low coverage was studied by total-energy LDF calculations. The adsorption geometry of Na and K atoms on the Si(001) surface was found to be strongly field-dependent. In contrast, the adsorption geometry of Sb on the Si(001) surface was almost insensitive to the field. The different topographic and electronic responses of different atoms in the surface resulted in changes in the relative contrast of the adsorbed atoms and the substrate in STM images. The calculated filled-state images were found to be similar to reported experimental images [Y.W. Mo, Phys. Rev. Lett. 65 (1990) 3417; A. Brodde, Th. Bertrams, H. Neddermeyer, Phys. Rev. B 47 (1993) 4508]. We found that the electric field inhibits empty-states imaging of alkali metals on Si(001) surface. Possible distortions of the tunneling spectra are discussed. Our results demonstrate that the tip-induced electric field is an important factor in forming STM data, and cannot be neglected in the interpretation of STM images and spectra. © 1997 Elsevier Science B.V.

Keywords: Alkali metals; Antimony; Chemisorption; Density functional methods; Silicon; Surface relaxation and reconstruction

1. Introduction

The ability of scanning tunneling microscopy (STM) to image individual atoms makes it a powerful tool for investigating adsorption processes. Nevertheless, the information obtained from STM images and spectra is usually compared with results of other experimental techniques or calculations [1–23] to achieve maximum reliability. As will be shown here, another reason for such caution is the effect of the electric field. Usually, the assumption is that the STM measurement does not affect the atomic positions and the local electronic structure of the sample. This assumption originated from early theories where the tip and the sample were considered to be completely non-interacting. In reality, however, the tip induces an electric field of the order of 0.1 V Å^{-1}. Several attempts were made to include the bias voltage in calculations of STM images and spectra [18–21]. In most of these calculations, the voltage was considered in the calculation of the current but the unperturbed electronic structures of the tip and the sample were used. Recently, Hirose and Tsukada [20] have carried out first-principles calculations for a bimetallic junction under a strong field and current. They found that the electronic structure of both electrodes is significantly affected by the field.

For semiconductor surfaces, the atomic positions may also be affected. The effect of the tip-

* Corresponding author. Fax: +972 8 9344123; e-mail: cimanas@weizmann.weizmann.ac.il

PII S0039-6028(97)00162-3

induced electric field on the atomic and electronic structure was discussed for a clean Si(001)-(2 × 1) surface [6–8,10]. It was shown that the external electric field caused additional relaxation in the clean Si(001)-(2 × 1) reconstruction. According to one calculation, the atomic positions and the electronic structure of the Si dimers are only slightly distorted even by a strong field [6]. Others have found that STM images and spectra can be understood only by taking into account the significant dependence of the dimer buckling on the polarity of the tip-induced field [7,8,10].

The presence of adsorbed atoms causes further complications. The atomic position and electronic structure are affected, even for metal atoms adsorbed on metals [24,25]. In this system the external field is almost completely repelled from the adatom-surface region. In semiconductors the external field penetrates inside the bulk up to 0.5 μm, and therefore this effect should be more pronounced. Obviously, the field-induced changes in the adsorption geometry and local electronic structure depend on the adsorbate, the type of bonding and the magnitude and direction of the field.

The models of atomic adsorption are calculated as the lowest-energy configurations. In comparing such models with STM images, the possible distortion of the adsorption geometry as a result of the tip-induced field is not taken into account. For group-V elements such as antimony or arsenic, the calculated adsorption configurations agree with the STM images. In contrast, for adsorption of alkali metals (AM) on Si(001), both the adsorption geometry and the bonding type are still a subject of discussion. The proposed degree of the AM ionization varies from 0 to 1 [3,13,26,27]. In all reported filled-state images of AM on Si(001), the AM atoms are seen as bright spots, indicating that they are not completely ionized [32,33]. The sole reported atomically resolved empty-state image of K/Si(001) does not show distinct K-related features [33]. To explain the absence of empty-state images, it was proposed that the AM atoms are captured by the negatively biased tip. Johansson et al. [23] recently reported on the first tunneling spectrum of filled states for Li/Si(001). No scanning tunneling spectroscopy (STS) data for other AMs were reported.

Here we present our total-energy local-density functional (LDF) study of the influence of the tip-induced electric field on STM images and spectra of Sb, Na and K adsorbed on a Si(100) surface. We found that the electric field induces relaxation in clean and covered Si surfaces, the degree of relaxation varying for different atoms. The non-uniform topographic and electronic responses result in changes in the relative contrast of the adatoms and the substrate in the STM images. This significant relaxation also affects the local density of states (LDOS), and consequently the tunneling spectra. Such spectra cannot therefore be compared directly with calculated LDOS or with spectra obtained by other spectroscopic techniques. The surface response to the tip-induced electric field must be considered when STM/STS data are interpreted.

2. Model

We used an ab initio all-electron numerical total energy DMOL method [28] with the Hedin–Lundqvist/Janak–Morruzi–Williams local correlation and the Beske gradient-corrected exchange functionals for calculating the geometric and energetic properties of the surface. For all atoms, a double numerical basis set with a frozen core approximation for the 1s2s orbitals of Si and Na and the 1s2s2p orbitals of Sb and K was used.

For each set of calculations, a cluster with the appropriate geometry was constructed. The asymmetric dimer configuration was used as the starting geometry of the substrate. For all clusters, C_{2v} symmetry was assumed to reduce the number of calculations, which sometimes restricted the geometry relaxation. A test study for large clusters using low symmetry (C_s and C_i) showed that this limitation does not significantly affect the results. All broken bonds (except the surface dangling bonds) were saturated with hydrogen atoms which were fixed in their positions during geometry optimization. In each calculation the geometry of the cluster was relaxed to minimize the total energy of the system. The conversion criterion was 1×10^{-6} Ry

for the energy and 1×10^{-3} Ry a.u.$^{-1}$ for the energy gradient.

The external electric field penetrates substantially into the semiconductor. Thus, only part of the full tip–sample potential drops across the vacuum (Fig. 1). The penetration depth of the external field depends on both the bulk properties of the semiconductor (such as the doping level) and the surface properties (such as the presence of surface states inside the bandgap). In order to estimate correctly the electric field (E_{vac}) produced by the tip in the vacuum region, the buffering role of the semiconductor bulk should be considered: $E_{vac}=(V_b-V_s)/d$, where V_b is the bias voltage, d is the distance between the tip and the surface, E_{vac} is the electric field in the tunneling region, and V_s is the surface potential. For a semiconductor without surface states inside the gap, the field-induced surface potential is defined by the polarity and the strength of the field and by the penetration length $L_D=(\epsilon kT/4\pi e^2N)^{1/2}$, where ϵ is the dielectric constant of the semiconductor, e is the charge of the electron and N is the doping level. Since we are interested in the order of magnitude of the surface potential induced by the strong external electric field, we can use a simplified approximation

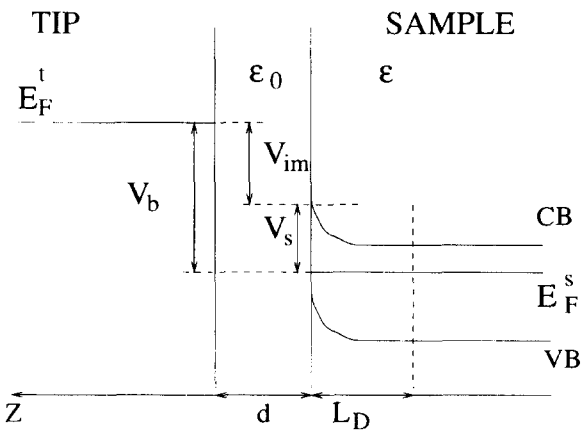

Fig. 1. The partition of the bias voltage V_b between the vacuum region and the semiconductor. V_s is the surface potential, V_{im} is the actual imaging voltage, ϵ_0 and ϵ are dielectric constants of the vacuum and the semiconductor, respectively, E_F^t and E_F^s are the Fermi levels of the tip and the sample, respectively, CB and VB stand for the conduction and valence bands of the sample, d is the width of the tunneling gap, and L_D is the penetration length.

for V_s [29]: $V_s=E_{vac}L_D/\epsilon$. For the n-type silicon without surface states, with a doping level of 10^{-18} cm^{-3} and a biased tip (-1 V) 5 Å above the surface, E_{vac} is estimated to be 0.12 V Å^{-1}.

The presence of surface or defect states can restrict the field-induced band bending or, if the density of surface states is large enough, completely pin the Fermi level. Here, the surface potential is independent of the doping level and is much smaller than in surfaces free of surface states. The surface Fermi-level pinning effectively screens the space-charge region of the semiconductor from the external field; however, the outermost layers are still affected by the field E_{vac}. Interaction of the surface with an adsorbed atom usually removes or changes the amount of surface states in the vicinity of the adatom. Therefore, V_s is the local property of the surface. The difference between the bias voltage V_b and V_s is the actual imaging voltage (V_{im}) which defines on a microscopic scale the energy states participating in tunneling; it also defines the local value of E_{vac}. The simplified calculation of E_{vac} may underestimate the real field. Therefore, the effect of the electric field is probably larger than that estimated in this paper.

The STM tip can be considered as a metal plate with a small cluster on it. The cluster causes an enhancement of the electric field just below it [24]. For typical distances used in STM (about 5 Å), this field enhancement will not exceed 30% of the uniform field. Here, only the uniform field component was considered. For each cluster, a set of five calculations were performed, without an external field and in the presence of uniform electrostatic fields: ± 0.1 and ± 0.2 V Å^{-1}. Two additional calculations were carried out with ± 0.3 V Å^{-1} for K/Si(001). A positive direction of the electric field is oriented from the surface towards the vacuum. In the experiment, it corresponds to tunneling from the tip into empty sample states.

Using these data, local density of states (LDOS) energy spectra ($d\ln I/d\ln V$ versus V) graphs and constant-current images were calculated. A peak width of 0.2 eV was used for the LDOS spectra. The origin for the spectra was placed at the middle of the HOMO–LUMO gap. To mimic the tip's electronic structure near the Fermi level (d- and s-bands), a sum of two normalized Gaussians of 1

and 3 eV width with the same origin was used. To simulate the tip–sample energy overlap for calculations of the current, the surface LDOS was convoluted with the model tip LDOS located at eV_b (V_b is the bias voltage) with respect to the surface Fermi level. Both the sample and tip LDOS were broadened by a Fermi distribution corresponding to room temperature. For calculation of STS, the current was averaged over the unit cell.

STM images were simulated by combining the current distribution calculated at a distance of 4 Å above the upper dimer atom for the clean surface and above the adsorbed atom for the covered surface. The composed picture was then converted to a constant-current image using the exponential dependence of the current on the tunneling distance.

3. Results and discussion

First, the optimized geometries for a clean Si(001) surface and for a surface covered with either Sb, Na or K were calculated. The clean Si(001) surface was studied with clusters containing one dimer ($Si_{17}H_{20}$), two dimers from parallel rows ($Si_{31}H_{34}$) and four dimers for a p(2×2) reconstruction ($Si_{53}H_{44}$). For the double-dimer cluster, two equally stable structures corresponding to correlated out-of-phase buckling were found. For this cluster, the in-phase buckled structure was not even a local minimum, and was spontaneously converted to either of the stable structures during optimization. A four-dimer cluster exhibits two stable structures (Fig. 2), corresponding to c(4×2) and p(2×2) reconstructions, the former being only slightly more stable (by 0.01 eV per dimer), which is in good agreement with STM observations and recent dynamics calculations [22].

Antimony atoms at low coverage are thought to be adsorbed on Si(001) as dimers sitting on top of the Si dimer rows and oriented perpendicularly to the underlying Si dimers. To simulate this surface, we used a $Si_{15}H_{20}Sb_2$ cluster with alternatively buckled asymmetric Si dimers. After optimization, the buckling of the dimers disappeared completely. In the underlying Si layer the unreconstructed geometry was almost restored, although the Si dimer atoms remained closer to each other than in the ideal surface (3.62 Å instead of 3.84 Å). The calculated Sb dimer bond length is slightly larger than the experimental value. Nevertheless, the geometry obtained agrees reasonably with the experimental results.

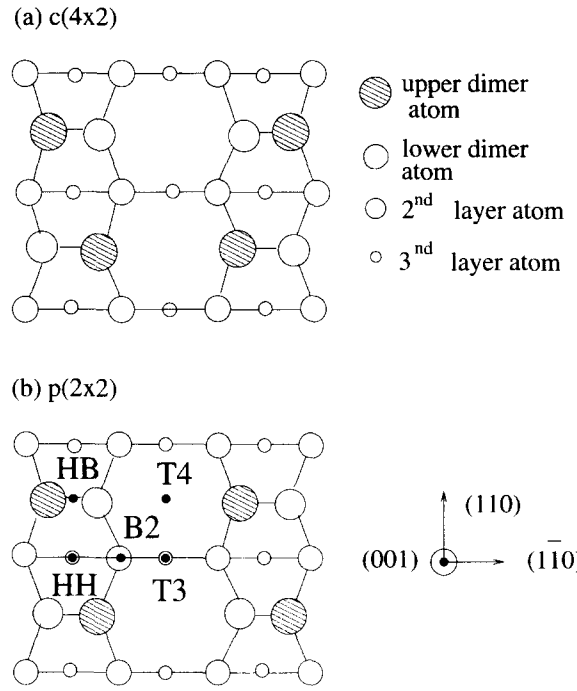

Fig. 2. The c(4×2) (a) and p(2×2) (b) stable reconstructions of the Si(001) surface. The shaded circles denote upper dimer atoms. In (b) the adsorption sites for alkali metal atoms on Si(001)-c(4×2) surface are marked by small filled circles. The acronyms T4, T3, HH, HB and B2 denote the cave, valley bridge, pedestal, dimer bridge and intermediate bridge sites, respectively.

Fig. 2b shows the adsorption sites for the adsorption of AM on Si(001). Several calculations [3,13,17,30] show that the cave and the valley bridge sites are close in adsorption energy and are more stable than other sites. A photoemission extended X-ray absorption fine structure (EXAFS) study of Na/Si(001) [9] confirmed adsorption on the cave site, whereas pseudo-potential calculations [13,30] proposed that the valley bridge site is slightly more stable than the cave site. Alternatively, recent surface EXAFS measurements of K/Si(001) [31] suggested low-symmetry

dangling-bond sites, where the potassium atom located between the rows is bound either to one dimer atom or is bridging two adjacent atoms in the row. A close look at the proposed structures reveals that they are equivalent to the cave and the B2 site. The B2 site has already been ruled out by calculation as being less stable [13,30]. Another parameter which is still unclear is whether the Si dimers are symmetrized upon adsorption. Symmetrization of the dimers was proposed for saturation coverage [13,30], and is frequently used in the analysis of structural measurements for submonolayer coverage. However, Ko et al. [30] showed that for Na atoms adsorbed at low coverage, buckling of the surface dimers persists.

To define the adsorption site for Na and K atoms, we studied the relative stability of the cave and valley bridge sites. The $Si_{31}H_{32}Na(K)$ cluster for the cave site and the $Si_{53}H_{44}Na(K)$ cluster were used for the valley bridge site. The adsorption energy of the AM atom was calculated as the difference between the binding energies of the corresponding cluster with and without the AM atom. The bond length was defined as the shortest distance between the AM and the Si atoms. Adsorption energies at the cave site for both Na and K atoms were found to be larger compared to the valley bridge site, and the calculated bond length for adsorption at the cave site agrees better with the experimental values (see Table 1). Therefore, in further calculations only the cave site was considered. In both structures the surface dimers remain buckled towards the AM atom, although buckling is reduced compared to the clean surface. Symmetrization of the dimers is more prominent upon K adsorption. Fig. 3 shows the different clusters used in calculations. Table 2 summarizes some parameters of the optimized structures.

Table 1
The AM–Si bond lengths $L_{Na(K)-Si}$ (in Å) and adsorption energies E_a (in units of eV per atom) for cave and valley bridge adsorption sites

	Valley bridge T3	Cave T4	Experiment
K $L_{K\ Si}$	3.87	3.46	3.20 ± 0.02[a]
E_a	2.03	2.23	
Na L_{Na-Si}	3.46	2.86	2.67 ± 0.05[b]
E_a	2.21	2.48	

[a]From Ref. [31].
[b]From Ref. [9].

The geometry and the electronic structure of the clean and Sb-, Na- and K-covered Si surfaces were calculated in the presence of an external electric field. Fig. 4 shows the changes in the adsorption geometry induced by the field. The difference in the response to the applied field between the different adatoms and the underlying Si layer is remarkable. The relaxation of the Sb dimer geometry is smaller than that of the clean surface dimers, whereas the changes in AM atom positions are an order of magnitude larger than those of the clean surface. Interestingly, the behavior of Na- and K-covered surfaces is different. In the Na-covered surface, the underlying Si dimers are only slightly affected. The amount of buckling does not change with the field. The average dimer height varies in the order of 0.01 Å. In contrast, there are drastic changes in the geometry of the Si dimers on the K-covered surface. The buckling of the dimers increases greatly for a positive field; for a negative field the increase in buckling is smaller. Note that the direction of the relaxation of the atoms is defined by their effective charge. The upper dimer atom in the clean Si surface is negatively charged because of charge transfer in the buckled dimer. Sb, Na and K atoms are positively charged. With K/Si(001), the relaxation of surface dimers is not related to the electrostatic interaction with the tip, but to the elastic force applied by the relaxed potassium atom.

The penetration of an external electric field inside the semiconductor causes a shift in the surface LDOS position. The surface LDOS response to the electric field depends on whether a covered or a clean surface is considered. The LDOS spectra have a general trend to shift up for a positive field and down for a negative one, but the shift itself differs from peak to peak (Fig. 5). The field-induced changes in the bonding between the adsorbed atom and the surface are reflected in the behavior of the mixed adatom–Si states.

For the Sb-covered surface, the occupied (A1,

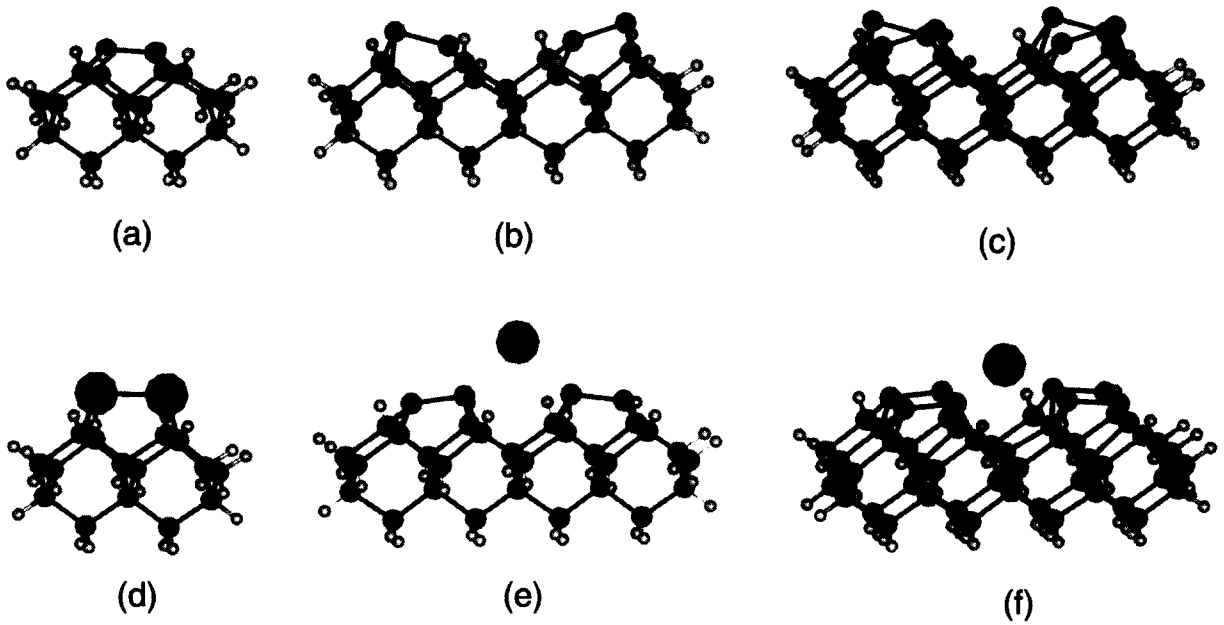

Fig. 3. Ball-and-stick models for the clusters used in the calculations. (a)–(c) The optimized structure of the clusters representing the clean Si(001) surface: (a) the one-dimer $Si_{17}H_{20}$, (b) the double-dimer $Si_{31}H_{32}$ and (c) the four-dimer $Si_{53}H_{44}$. For the covered surface: (d) the $Si_{15}H_{20}Sb_2$ cluster representing the Sb/Si(001), (e): the $Si_{31}H_{32}Na(K)$ clusters representing the cave adsorption site, and (f): the $Si_{53}H_{44}Na(K)$ clusters representing the valley bridge adsorption site.

A2) and the empty (B, C) Sb $5p_z$–Si $3sp^3$ states are uniformly shifted for both polarities of the field (Fig. 5a). The energy shift of the spectrum is a result of the external field only. This reflects the fact that the adsorption geometry of Sb/Si(001) is hardly affected by the field.

In K- and Na-covered surfaces, the external field strongly shifts the AM valence s-state. Consequently, the energy overlap changes between AM s-orbitals and Si orbitals available for bonding. In addition, the geometric relaxation causes changes in the spatial overlap between these orbitals. Both of these factors affect the LDOS.

In Na/Si(001), the Si surface states (A, B) and the dimer σ^* state (C) are slightly mixed with the Na 3s orbital when no field is applied (Fig. 5b). In a negative field, the Na atom moves closer to the surface and the energy if its valence s-orbital decreases. As a result, both the spatial and energy overlaps increase. The intensity of all these peaks increases as the contribution of the Na 3s orbital grows. For a positive field, the Na 3s orbital is greatly shifted to higher energies. At the same time the Na atom is pulled out from the surface. The contribution of the Na 3s orbital to the mixed states decreases, but some overlap still remains. The high-lying Si 3p states overlap with the strongly shifted Na 3s state. The intensity of the empty LDOS states changes upon increasing the field, and the peak assignment also changes. However, the surface dimer σ state (peak D in Fig. 5b) is almost unaffected, which indicates that in the Na-covered surface the silicon dimers are only slightly affected.

For the K-covered surface, the field-induced relaxation of the surface dimers complicates the effect of the field on the LDOS. The dimer σ-state is shifted to higher energies for both field polarities, as the dimers become more buckled (peak D in Figs. 5c and 5d). For the positive field, the intensity of all dimer-related states (A–D) decreases because of a weakening of the dimer bond. The changes in the empty Si states are defined by both the external field and the structural rearrangement. As a result, apparently similar LDOS peaks have a different assignment (E and F in Fig. 5c). The contribution

Table 2
Parameters of the optimized structures used for the calculations (in Å)

	Calculated	Experimental
Clean Si(001)		
L_d[b]	2.52	2.47[g]
ΔZ[c]	0.73	
Sb/Si(001)		
$L_{Sb\text{-}Sb}$[d]	3.16	2.88±0.03[h]
$L_{Sb\text{-}Si}$	2.75	2.66±0.03
h_{Sb}[e]	1.83	1.74±0.03
Na/Si(001)[a]		
$L_{Na\text{-}Si}$[f]	2.86	2.67±0.05[i]
L_d	2.43	2.44±0.04
ΔZ	0.35	
K/Si(001)[a]		
$L_{K\text{-}Si}$[f]	3.46	3.20±0.02[j]
L_d	2.31	
ΔZ	0.20	

[a]Na and K parameters are for adsorption on the cave site.
[b]L_d denotes the dimer bond length.
[c]ΔZ denotes the extent of dimer buckling (the height difference between the upper and the lower atom in the dimer).
[d]$L_{Sb\text{-}Sb}$ denotes the Sb–Sb distance.
[e]h_{Sb} denotes the height of the Sb atom above the surface.
[f]$L_{Sb\text{-}Si}$ and $L_{Na(K)\text{-}Si}$ denote the smallest distance between the adatom and the Si atoms.
[g]From Ref. [35].
[h]From Ref. [11].
[i]From Ref. [9].
[j]From Ref. [31].

of the K 4s orbital to the filled state (A), which is almost negligible when no field is applied, greatly increases for a negative field (Fig. 5e), as in Na/Si(001). For a positive field it provides the main contribution to the A and B peaks.

The effect of the electric field on the surface to some extent restricts the capability of STM imaging and spectroscopy to be a reliable local probe for the surface LDOS. This effect is complicated because the tip-induced field increases with the voltage. The extent of this limitation depends on the field sensitivity of the electronic structure in a specific system.

Since both the local atomic and electronic structures of the surface contribute to forming an STM image, it is expected that the images will also be affected by the field. Before discussing the simulated images, we will define the actual imaging voltage used in the calculation. In an experiment, the actual imaging voltage is smaller than the bias voltage applied between the tip and the sample, and can vary within the imaged area (Fig. 1). For calculations of the images we used the same value (−2 V) of the actual imaging voltage for the whole image, taking into account the variation of the Fermi-level position only in calculating the local barrier height. The consequences of possible differences in the actual imaging voltage will be discussed later.

Fig. 6 shows the simulated images of Sb on Si(001) without an external field and with a field of $-0.2\ \mathrm{V\ \AA^{-1}}$. Both images were calculated for the same value of the current. Two characteristic features appear with the field: (i) the corrugation on the clean surface becomes smaller, which can be attributed to the increasing contribution of the Si dimer σ-bond which is spatially more spread between dimer rows, and (ii) the relative height of the Sb dimer increases, which is an electronic consequence of the topographic response: as the Sb dimer moves slightly closer to the underlying Si (Fig. 4), the intensity of the bonding state (A2) increases (Fig. 5a). Even a minor response of the surface to the applied field will affect STM images (compare with Fig. 2 in Ref. [12]).

We now consider K/Si(001), the system with a larger field sensitivity. Figs. 7a and 7b show simulated filled-state images with and without an electric field. The difference between the two images in the vicinity of the K atom is apparent: when no field is applied, the K atom is not seen. The relative height of the dimers nearest to the potassium atom increases because of the smaller barrier height in this region. The individual rows are clearly seen. When a negative field is taken into account, the K atom is imaged as a large protrusion between the dimer rows. The appearance of this protrusion is purely an electronic effect. Indeed, the K atom moves towards the surface (Fig. 4). On the other hand, its contribution to the A state becomes significant (Fig. 5e). The A state defines the main features of the image, and the K atom becomes visible at its true position between the rows. The images shown in Figs. 7a

(a)

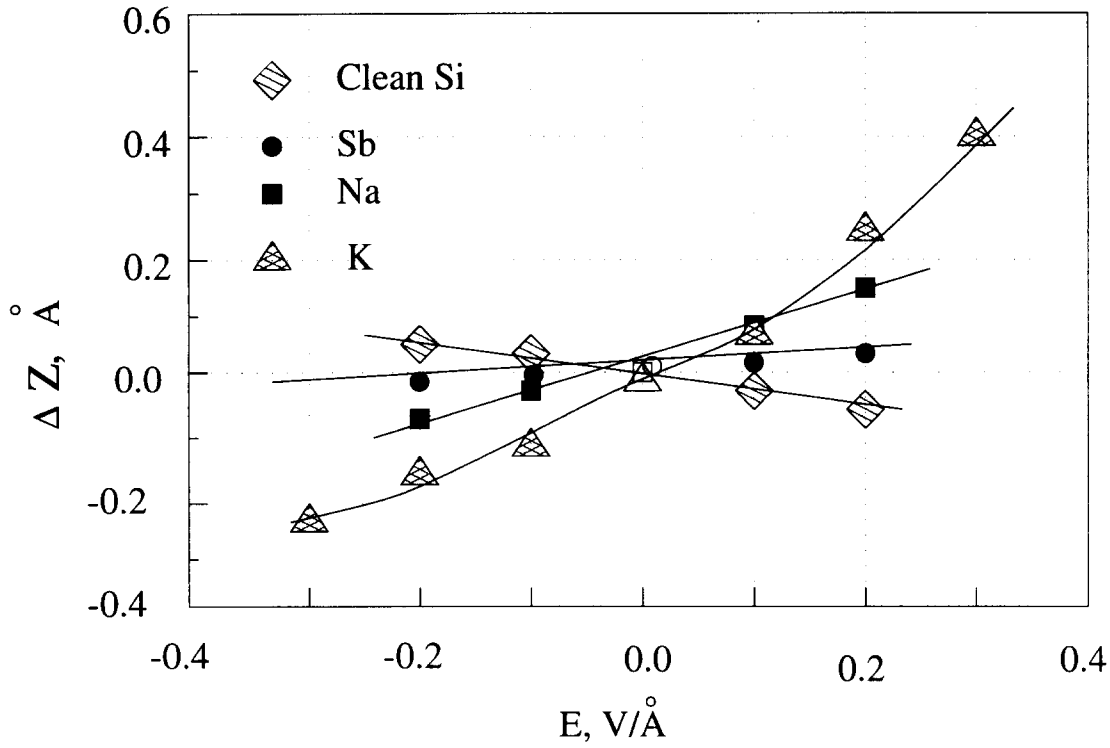
0.6
0.4
0.2
0.0
-0.2
-0.4
Clean Si
Sb
Na
K
Δ Z, Å
-0.4
-0.2
0.0
0.2
0.4
E, V/Å

(b)

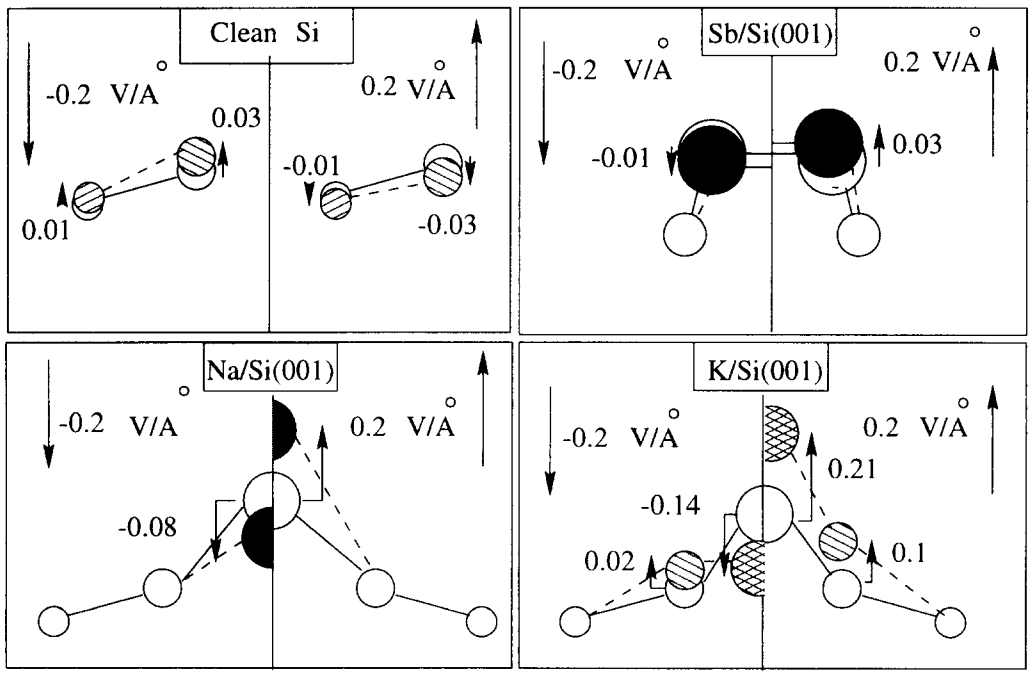
Clean Si
-0.2 V/A
0.2 V/A
0.03
0.01
-0.01
-0.03
Sb/Si(001)
-0.2 V/A
0.2 V/A
-0.01
0.03
Na/Si(001)
-0.2 V/A
0.2 V/A
-0.08
K/Si(001)
-0.2 V/A
0.2 V/A
0.21
-0.14
0.02
0.1

and 7b were calculated with a voltage of −2 V. The images calculated with a voltage of −1.4 V are similar to those calculated with −2 V. The only difference is in the absolute value of the current. Comparing with the experimental images in Figs. 7e and 7, the image calculated without electric field (Fig. 7a) is similar to the experimental image (Fig. 7e) taken with a voltage of −1.4 V (weaker field expected). The image calculated with the field (Fig. 7b) agrees with the image (Fig. 7f) taken with a voltage of −2 V (stronger field expected).

For the positive field, the actual imaging voltage (V_{im}; see Fig. 1) becomes an important factor. The K atom causes local metallization of the surface because of partial filling of Si surface states. Consequently, the whole bias voltage acts as the imaging voltage. Thus, E_{vac} in this region is stronger relative to that in the surrounding surface. A K atom at a field of $+0.3\ V\ Å^{-1}$ is pulled out by 0.4 Å (Fig. 4). Thus, at working bias voltages of about 2 V, potassium can easily be picked up by the tip. Indeed, difficulties in observing empty-state images were reported for all AMs on Si(001).

A knowledge of the field sensitivity of a particular adatom–surface system is thus crucial for the interpretation of STM images. The field-assisted imaging of filled K states is not a unique example. The non-uniform topographic and electronic response of the covered surface to the field suggest a direct application: the changes in the relative contrast of the free surface dimers and adsorbed atoms with increasing voltage can be used for identifying defects and adatoms. An example of such an application has already been demonstrated. It was shown that imaging with an increasing negative voltage enables the discrimination of H-saturated dimers from true vacancies on the Si(100)-H surface [15]. Finally, the effect of the electric field on STS must be mentioned. STS data are taken in variable field conditions. The measured normalized conductance ($d\ln I/d\ln V$) is thought to be a good approximation for the sample LDOS. In the frame of our simple model of the tip LDOS, this is indeed true if the spectra are calculated using zero-field LDOS (Fig. 8). When the variable field was included in the calculation, the relation between the sample LDOS and the normalized conductance became more complicated. The simulated spectrum of Sb/Si(001) (Fig. 8a) appears unaffected by the field. The peak assignment remains unchanged. For Na/Si(001) (Fig. 8b), the spectrum of the filled states is also unchanged. However, for a positive field, the number of peaks does remain the same, but their assignment changes. For K/Si(001), all peaks are affected (Fig. 8c).

4. Conclusions

Using total-energy LDF calculations we studied the effect of the tip-induced electric field on the adsorption geometry and electronic structure of Sb, Na and K atoms adsorbed on the Si(001) surface at low coverage. Field-induced surface relaxation was found. The relaxation is 0.01–0.02 Å for clean Si(001) and for Sb/Si(001). In contrast, the adsorption geometry of AM atoms is very sensitive to the electric field; the position of both the AM atom and the nearest Si atoms is changed by 0.1–0.4 Å. The non-uniform response of the clean and covered Si(001) surfaces to the applied field leads to changes in relative contrast in STM images taken under different field conditions. For field-sensitive systems such as AM/Si(001), imaging might even be inhibited, depending on the polarity of the bias voltage. The dependence of the relative contrast on the electric field may also be used to discriminate between native defects of the clean surface and adsorbed atoms.

STS data correspond to variable field conditions, and may therefore differ significantly from calcu-

Fig. 4. The field-induced geometry relaxation. (a) Changes in the Z-coordinate of the adsorbed atoms and the upper dimer atom of the clean surface. (b) The details of the relaxation of the adsorption geometry. The open circles represent the zero-field structure, and the shaded circles represent the relaxed structure. If the atom did not move during relaxation, the circle is empty for both structures. The direction and the magnitude of the fields are shown in each panel. Changes in the atomic positions relative to the zero-field structure (in units of Å) are shown by numbers.

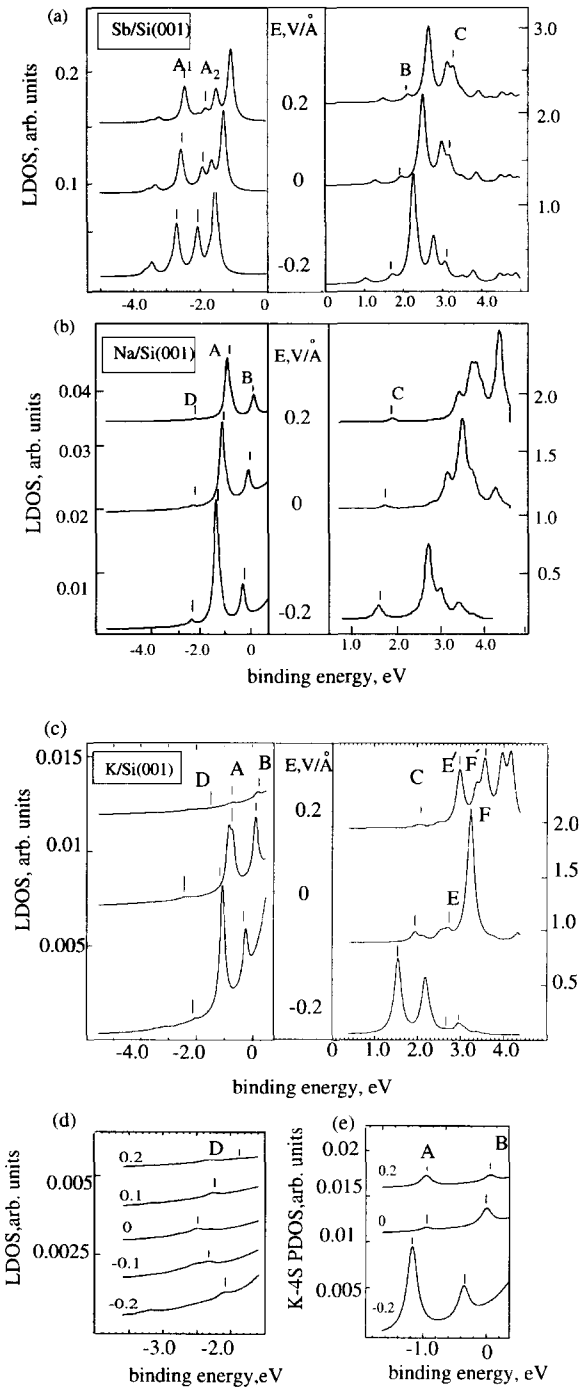

Fig. 5. The evolution of the LDOS in the external electric field for (a) Sb/Si(001), (b) Na/Si(001), (c) K/Si(001). In (a), A_1, A_2, B and C denote mixed Si–Sb states. In (b) and (c), A and B denote the surface states (dimer π and π^* states), while C and D denote the Si dimer σ^* and σ states. Other peaks in (c) are: E, Si 3s–K 4s; E′, Si 3s; F, K 4s; F′, Si $3p_z$–K 4s. Note the different scale in each panel. (d) The evolution of the dimer s-bond for K/Si(001) (peak D) in more detail, and (e) the evolution of the partial DOS for the K 4s orbital. Lines corresponding to different values of the electric field are shifted for clarity.

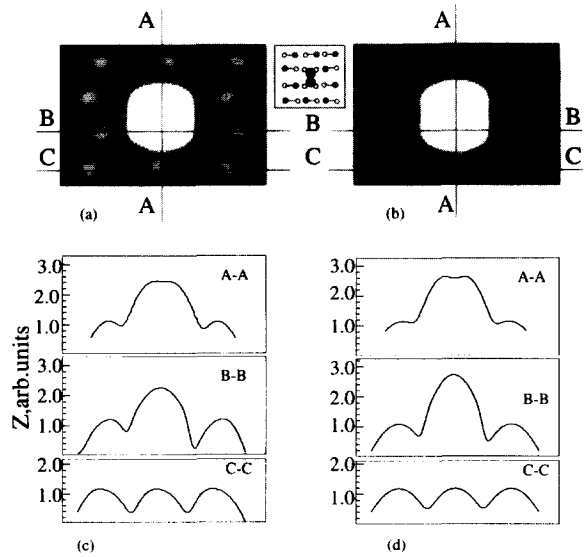

Fig. 6. Simulated filled-state STM images of Sb/Si(001) (a) without an electric field and (b) with a field of $-0.2\,\mathrm{V\,Å^{-1}}$. The registry of the surface dimers is shown in the inset. Small open circles denote low dimer atoms, small filled circles denote upper dimer atoms and large shaded circles denote Sb atoms. In (c) and (d) the cross-sections along marked lines are shown.

lated LDOS or spectra obtained by other spectroscopic techniques. Variable separation spectroscopy [34] partially solves this problem, increasing the range of voltages which produce a relatively weak field. Nevertheless, the linear dependence of the induced field on the tip voltage is not fully compensated by increasing the distance. In analysis of tunneling spectra, taken either with variable or constant field conditions, the non-uniform response of surface LDOS to the applied field should be taken into account.

Our results show that the tip-induced electric field is an important factor in the forming of STM data, and cannot be neglected in interpretation of STM images and spectra.

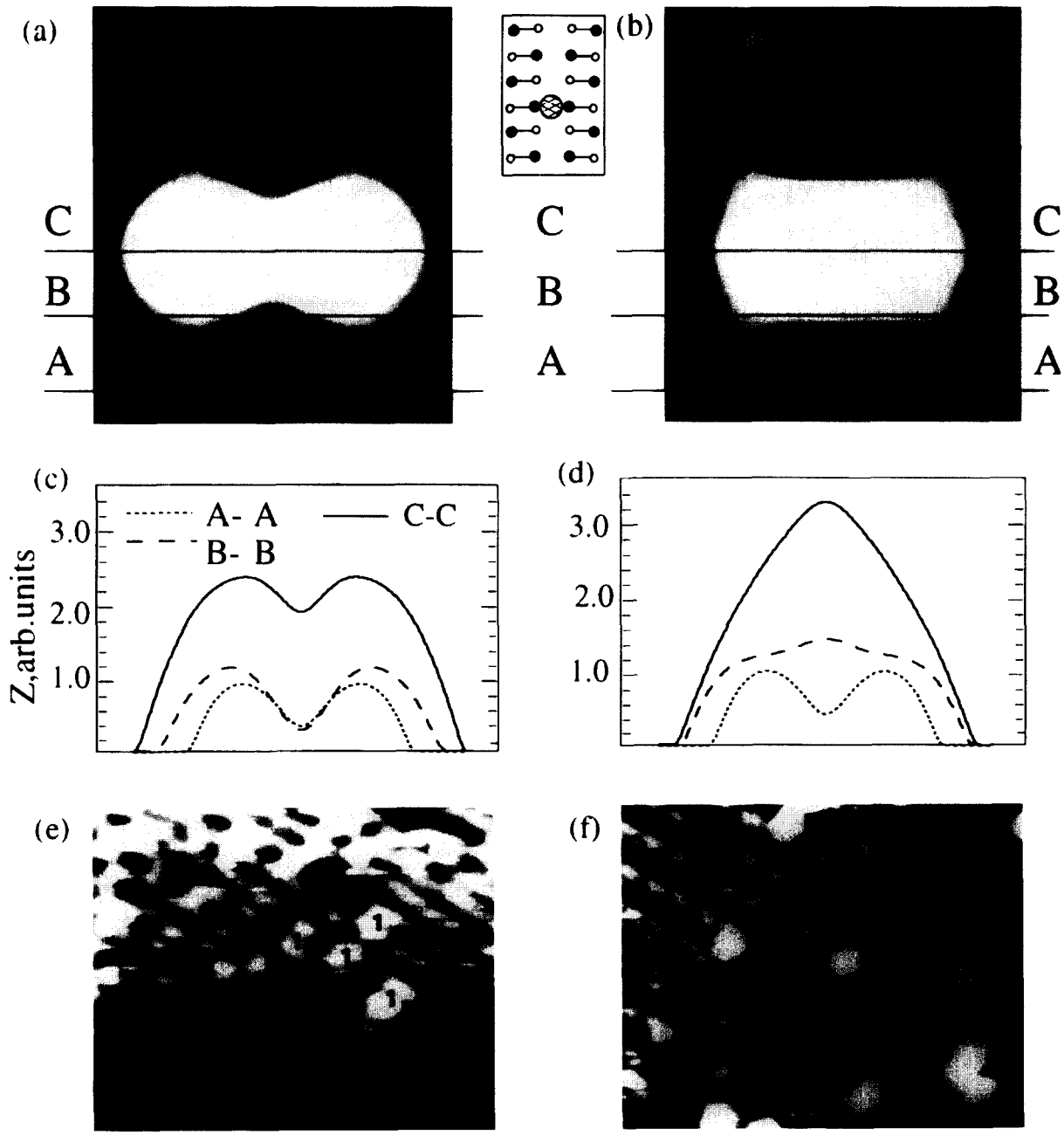

Fig. 7. Simulated filled-state STM images of K/Si(001) (a) without an electric field and (b) with a field of -0.2 V Å^{-1}. The registry of the surface dimers is shown in the inset. In (c) and (d) the different cross-sections of the image are shown. Experimental images taken with voltages of (e) -1.4 V and (f) -2 V are shown for comparison (from Ref. [33], with permission). Adsorbed K atoms are marked as 1 in (e) and as 2 in (f).

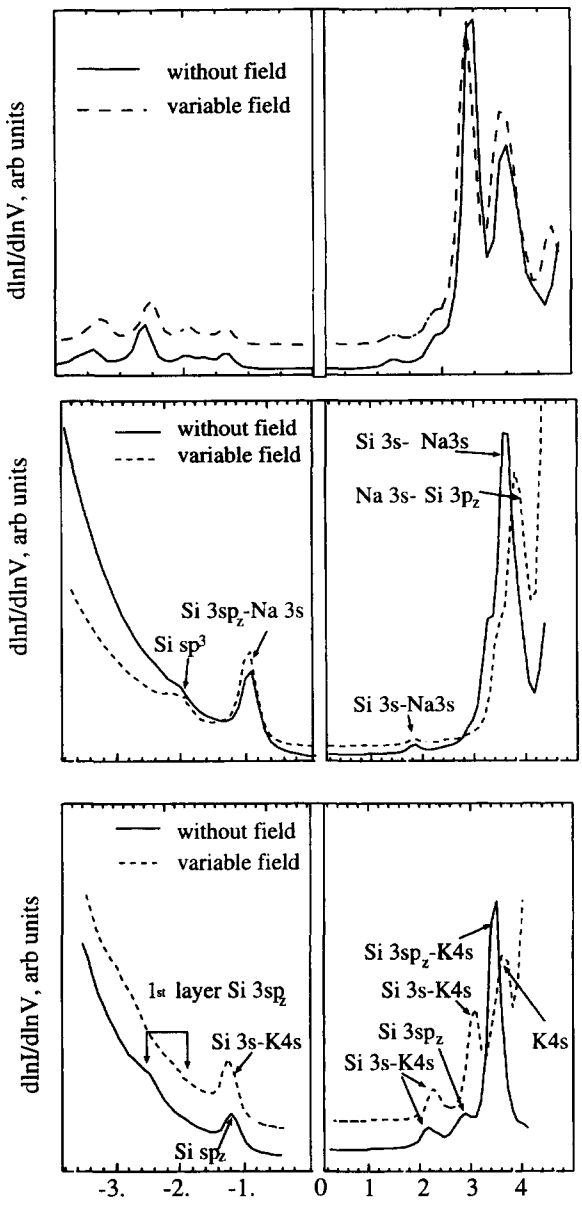

Fig. 8. Simulated tunneling spectra for (a) Sb/Si(001), (b)Na/Si(001) and (c) K/Si(001). The states which mainly contribute to the corresponding peaks are marked. Spectra corresponding to different field conditions are shifted for clarity.

Acknowledgements

We are grateful to Professor H. Neddermeyer for providing us with the original prints of the K/Si(001) images. This work was supported by the Minerva Foundation, Munich, Germany, by a grant from the Basic Investigation Foundation administered by the Israeli Academy of Sciences and Humanities, and by the Edith Reich Fund. Y.M. is an incumbent of the Lilian and George Lyttle Career Development Chair.

References

[1] R.S. Becker, T. Klitsner, J.S. Vickers, J. Microsc. 152 (1988) 157.
[2] R.I.G. Uhrberg, G.V. Hansson, Crit. Rev. Solid State Mater. Sci. 17 (2) (1991) 133.
[3] I.P. Batra, Phys. Rev. B 41 (1990) 5048; I.P. Batra, Phys. Rev. B 43 (1991) 12322, and references therein.
[4] K. Cho, J.D. Joannopoulos, Phys. Rev. Lett. 71 (1993) 1387.
[5] S. Tang, A.J. Freeman, B. Delley, Phys. Rev. B 45 (1992) 1776.
[6] Z.-H. Huang, R.E. Allen, Ultramicroscopy 42-44 (1992) 97; Z.-H. Huang, M. Weimer, R.E. Allen, H. Lim, J. Vac. Sci. Technol. A 10 (1992) 974.
[7] P. Badziag, W.S. Verwoerd, Surf. Sci. 285 (1993) 145; P. Badziag, W.S. Verwoerd, M.A. van Hove, Phys. Rev. B 43 (1991) 2058.
[8] Y. Hasegawa, I. Kamiya, T. Hashizume, T. Sakurai, H. Tochihara, M. Kubota, Y. Murata, Phys. Rev. B 41 (1990) 9688.
[9] L. Spiess, P.S. Mangat, S.-P. Tang, K.M. Schirm, A.J. Freeman, P. Soukiassian, Surf. Sci. 289 (1993) L631.
[10] M.M.D. Ramos, A.M. Stoneham, A.P. Sutton, J. Phys.: Condens. Matter 5 (1993) 2849.
[11] M. Richter, J.C. Woicik, J. Nogami, P. Pianetta, K.E. Miyano, A.A. Baski, T. Kendelewicz, C.E. Bouldin, W.E. Spicer, F. Quate, I. Lindau, Phys. Rev. Lett. 65 (1990) 3417.
[12] Y.W. Mo, Phys. Rev. Lett. 69 (1992) 3643.
[13] K. Kobayashi, Y. Morikawa, K. Terakura, S. Blügel, Phys. Rev. B 45 (1992) 3469.
[14] R. Souda, W. Hayami, T. Aizawa, Y. Ishizawa, Phys. Rev. B 47 (1993) 9917.
[15] Y. Wang, M.J. Bronikowski, R.J. Hamers, J. Vac. Sci. Technol. A 12 (1994) 2051.
[16] T. Kendelewicz, P. Soukiassian, R.S. List, J.C. Woicik, P. Pianetta, I. Lindau, W.E. Spicer, Phys. Rev. B 37 (1988) 7115.
[17] Y. Ling, A.J. Freeman, B. Delley, Phys. Rev. B 39 (1989) 10144.

[18] Y. Tersoff, Phys. Rev. B 40 (1989) 11990.
[19] M. Tsukada, K. Kobayashi, N. Issiki, H. Kadeshima, Surf. Sci. Rep. 13 (1991) 265.
[20] K. Herose, M. Tsukada, Phys. Rev. B 51 (1995) 5278.
[21] J.H. Wilson, D.A. McInnes, J. Knall, A.P. Sutton, J.A.B. Poetic, Ultramicroscopy 42-44 (1992) 801.
[22] A.I. Shkrebti, R.D. Felice, C.M. Bertoni, R. Del Sole, Phys. Rev. B 51 (1995) 11201.
[23] M.K.-J. Johansson, S.M. Gray, L.S.O. Johansson, Phys. Rev. B 53 (1996) 1362.
[24] H.J. Kreuzer, L.C. Wang, N.D. Lang, Phys. Rev. B 45 (1992) 12050.
[25] G.L. Kellogg, T.T. Tsong, Surf. Sci. 62 (1977) 343.
[26] H. Ishida, K. Terakura, Phys. Rev. B 40 (1989) 11519.
[27] L.S.O. Johansson, B. Reihl, Surf. Sci. 287/288 (1993) 524; Phys. Rev. B 47 (1993) 1401.
[28] B. Delley, J. Chem. Phys. 92 (1990) 508; 94 (1991) 7245; DMOL, Biosym Technologies, San Diego, CA.
[29] A. Many, Y. Goldshtein, N.B. Grover, Semiconductor Surfaces, part 4, Interscience, New York, 1965.
[30] Y.-J. Ko, K.J. Chang, J.-Y. Yi, Phys. Rev. B 51 (1995) 4329.
[31] R. Lindsay, H. Dürr, P.L. Wincott, I. Colera, B.C. Cowie, G. Thornton, Phys. Rev. B 51 (1995) 11140.
[32] T. Hashizume, I. Sumite, Y. Murata, S. Hyodo, T. Sakurai, J. Vac. Sci. Technol. B 9 (1991) 742.
[33] A. Brodde, Th. Bertrams, H. Neddermeyer, Phys. Rev. B 47 (1993) 4508.
[34] R.M. Feenstra, J.A. Stroscio, J. Vac. Sci. Technol. B 5 (1987) 923; P. Mårtinsson, R.M. Feenstra, Phys. Rev. B 39 (1989) 7744; J.A. Stroscio, R.M. Feenstra, J. Vac. Sci. Technol. B 6 (1988) 1472.
[35] B.W. Holland, C.B. Duke, A. Paton, Surf. Sci. 140 (1984) L269.